Effect of nitrogen addition to shielding gas on residual stress of stainless steel weldments

K. H. Tseng and C. P. Chou

The objective of the present study was to investigate the effect of nitrogen additions to the shielding gas on the ferrite content and residual stress in austenitic stainless steels. Autogenous gas tungsten arc (GTA) welding was applied on austenitic stainless steels 304 and 310 to produce a bead on plate weld. The delta ferrite content of the weld metals was measured using a Ferritscope. The residual stress in the weldments was determined using the hole drilling strain gauge method. The present results indicated that the retained delta ferrite content in type 304 stainless steel weld metals decreased rapidly as nitrogen addition to the argon shielding gas was increased. The welding residual stress increased with increasing quantity of added nitrogen in the shielding gas. It was also found that the tensile residual stress zone in austenitic stainless steel weldments was extended as the quantity of added nitrogen gas in the argon shielding gas was increased. STWJ/231

The authors are in the Department of Mechanical Engineering, National Chiao-Tung University, Hsinchu 30049, Taiwan (cpchou@cc.nctu.edu.tw). *Manuscript received 1 December 2000; accepted 11 January 2001.*

INTRODUCTION

Austenitic stainless steels, such as the type 300 series, are used in various types of plant, including heat exchangers, nuclear reactors, chemical processing equipment, and gas turbine parts, because of their excellent corrosion resistance, good mechanical strength at high temperature, and high fracture toughness at low temperature. However, austenitic stainless steels have higher thermal expansion coefficient and lower thermal conductivity than those of carbon or alloy steels. Therefore, a high magnitude residual stress can be induced after welding fabrication.[1]

Figure 1 shows schematically the process by which residual stresses are induced in the weldment during the welding process. A bead on plate weld is being deposited along the x direction. The heat source is moving at a velocity v, and is presently located at the point O, as shown in Fig. 1*a*. The crosshatched area M – M is the region where plastic deformation occurs during the welding process. The elliptical region near the origin O indicates the region where metal is melted. The region outside the crosshatched area experiences elastic deformation during the welding process.

Figure 1*b* shows the temperature distribution along several cross-sections. Section A – A is ahead of the heat source and is not yet significantly affected by the heat input. The temperature change ΔT due to welding is essentially zero (Fig. 1*b*, part 1). Along section B – B, which crosses the heat source, the temperature distribution has a rather high gradient (Fig. 1*b*, part 2). Along section C – C, which is some distance behind the heat source, the temperature distribution gradient becomes less steep (Fig. 1*b*, part 3). Along section D – D, which is a long distance from the heat source, the temperature change due to welding again diminishes to nearly zero (Fig. 1*b*, part 4).

Figure 1*c* shows the stress distribution in the x direction along the same sections. Along section A – A, which is not affected by the heat input, the thermal stress due to welding is almost zero (Fig. 1*c*, part 1). Along section B – B the stress is close to zero in the region underneath the heat source, since the weld pool cannot support a load. In the regions somewhat away from the heat source, stress is compressive because the expansion of these regions is restrained by surrounding metal that is at lower temperatures. Because the temperature of these regions is fairly high and the resulting yield stress of the base metal is low, stress in these regions reaches the yield stress of the base metal at the corresponding temperatures. The magnitude of the compressive stress increases with increasing distance from the weld or with decreasing temperature. However, stress in regions away from the weld is tensile and must be balanced with compressive stress in regions near the weld according to equilibrium conditions. Therefore, the stress distribution along section B – B is as shown in Fig. 1*c*, part 2.

Along section C – C, as shown in Fig. 1*c*, part 3, the weld metal and base metal regions near the weld have been cooled and hence have a tendency to shrink, thus producing tensile stress in regions close to the weld. As the distance from the weld increases, the stress first changes to compressive and then becomes tensile. The final residual stress condition for a bead on plate weld is shown in section D – D. Along section D – D, as shown in Fig. 1*c*, part 4, a high tensile stress is produced in regions near the weld, and compressive stress is produced in regions away from the

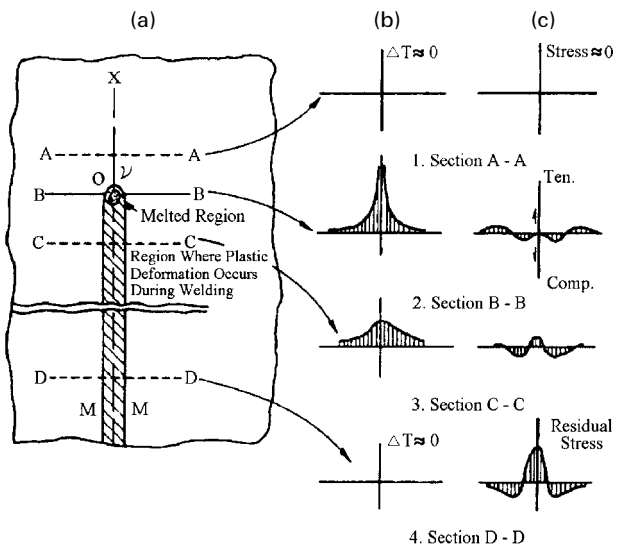

1 Schematic representations of *a* weld, *b* changes in temperature, and *c* changes in stress during welding process (after Refs. 2–5)

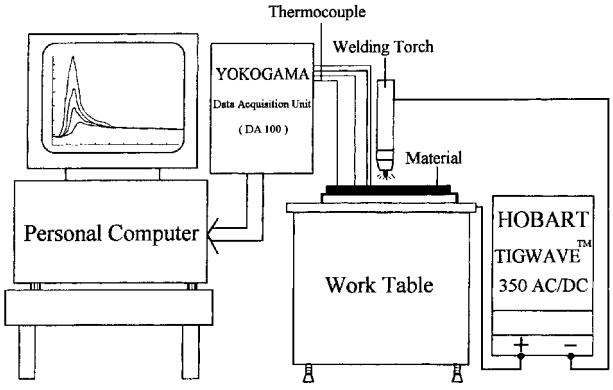

2 Thermal cycle recording system used

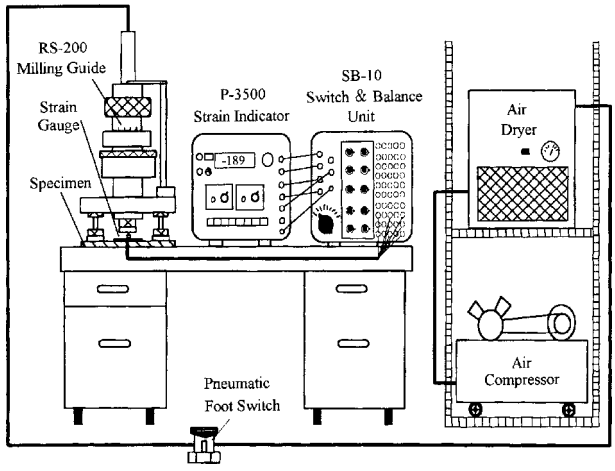

3 Residual stress measurement system used

weld. Since section D – D is well behind the heat source, the stress distribution does not change significantly beyond it, and this stress distribution is therefore the residual stress distribution.

In previous studies,[6–9] it was found that the welding residual stress can influence the mechanical and/or corrosion properties in service (such as brittle fracture, fracture toughness, fatigue strength, stress corrosion cracking, hydrogen cracking, etc.).

It is well known that nitrogen dissolves interstitially in austenite and is a strong austenite stabiliser. The stabilising effect of nitrogen is 20 to 30 times stronger than that of nickel,[10–12] and nitrogen has therefore been added to austenitic stainless steels to substitute for nickel as an austenite stabiliser. Incidentally, nitrogen addition to the shielding gas is used for certain alloys in arc welding practice. However, from the viewpoint of welding techniques, adding nitrogen gas to the shielding gas while maintaining strict control of the nitrogen content in the weld metal is fairly problematic. In gas tungsten arc (GTA) welding, electrode erosion has been found to result in excessive spatter and arc instability.[13]

It is widely known that nitrogen has the effect of increasing mechanical strength (such as ultimate tensile strength, yield strength, creep strength, and impact strength etc.),[13–18] improving pitting corrosion resistance,[14,19] etc. However, the study of the influence on the residual stress in weldments of additions of nitrogen gas to the argon shielding gas during the welding process has been limited. The aim of the present paper was to carry out detailed experiments to elucidate the effect of Ar – N_2 mixed gas on the delta ferrite content and residual stress in austenitic stainless steels. Furthermore, the relationship between the retained delta ferrite content and principal residual stress in austenitic stainless steels joined using GTA welding was also determined.

EXPERIMENTAL

Type 304 and 310 stainless steels were used in the present study. The chemical compositions and mechanical properties are presented in Table 1. To obtain the same initial stress state condition, test specimens having dimensions 130 × 130 × 8 mm were annealed at 950°C for 3 h before testing. The test specimens were roughly polished using 400 grit abrasive paper to remove surface impurity, then cleaned with acetone. Autogenous GTA welding was conducted using a standard 2% thoriated tungsten electrode. The electrode tip configuration was a blunt point with a 90° included angle. The welding processes were performed using pure argon and Ar – 2·5N_2, Ar – 5N_2, Ar – 7·5N_2, Ar – 10N_2, and Ar – 15N_2 (vol.-%) mixed gases. The shielding gas flowrate was 20 L min^{-1} for all compositions.

To record the thermal cycle of the weldments during GTA welding, a thermocouple was attached at 2 mm from the fusion line of the welds. The thermal cycle recording equipment included a dynamic temperature measurement system and a chromel – alumel thermocouple as shown in Fig. 2.

The ferrite number (FN) was measured using a calibrating magnetic instrument with a Ferritscope M10B – FE. To minimise the measured errors due to weldment inhomogeneity, the average value of seven measurements from different locations along the as welded surface was recorded.

After welding, a three element strain gauge rosette (Tokyo Sokki Kenkyujo Co., type TML FRS – 2 – 17) was attached at the centre location of the surface of the welds. A hole of diameter 1·6 mm was drilled using a hole drilling machine in the centre of the rosette to measure the residual stress of the weldment. The welding residual stress was determined using the hole drilling strain gauge method given in ASTM standard E837.[20] The welding residual stress measuring system is presented in Fig. 3.

The nitrogen contents in austenitic stainless steel weld metals were analysed using a Leco TC – 436 glow discharge optical spectrometer. Optical microscopy was used to examine the microstructure of the austenitic stainless steels after solidification. All metallographic specimens were prepared by mechanical lapping, grinding, and polishing to a 0·3 μm finish, followed by etching in a solution of 10 g $CuSO_4$ – 50 mL HCl – 50 mL H_2O.

RESULTS AND DISCUSSION

The welding parameters used in the present study are given in Table 2. The welding current, travel speed, and gas

Table 1 Chemical composition (wt-%, bal. Fe) and mechanical properties of austenitic stainless steels investigated

Steel type	C*	Si	Mn	P*	S*	Cr	Ni	Yield strength, MPa	Elastic modulus, GPa	Poisson's ratio
304	0·08	0·44	0·95	0·04	0·04	18·7	8·16	290	193	0·25
310	0·20	0·79	1·64	0·04	0·04	23·9	19·61	311	204	0·32

*Maximum values.

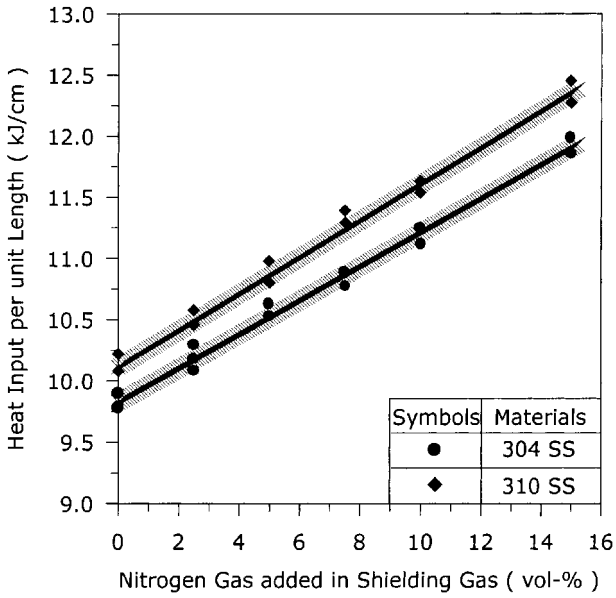

4 Calculated heat input as function of quantity of nitrogen added to shielding gas in gas tungsten arc (GTA) welding

flowrate were all fixed, with varying volume percentages of nitrogen gas added to the argon shielding gas during the GTA welding process.

Determination of initial stresses in test specimens

To evaluate the residual stresses induced after welding, the initial stresses in the test specimen were first measured using the hole drilling strain gauge method before welding. Table 3 gives the measured initial principal stresses for the base metals used. Since the values are fairly small, the initial stresses can be neglected in the present investigation.

Effect of nitrogen additions to shielding gas on heat input

Figure 4 shows the calculated heat input per unit length in GTA welds produced with various amounts of added nitrogen in the shielding gas. As the nitrogen addition to the argon shielding gas increases, the magnitude of the heat input is increased. This result can be related to the measured thermal cycle of the weldment during the GTA welding process as shown in Fig. 5. As the quantity of nitrogen added to the shielding gas increases, the peak temperature of the thermal cycle in the weldment is increased. This is

Table 2 Welding parameters for autogenous gas tungsten arc (GTA) welding process

Steel type	Current, A	Voltage, V	Travel speed, cm min^{-1}	Flowrate, L min^{-1}	Shielding gas
304	150	16·3	15	20	Pure Ar
		17·0			Ar–2·5N_2
		17·6			Ar–5·0N_2
		18·1			Ar–7·5N_2
		18·8			Ar–10N_2
		19·7			Ar–15N_2
310	150	16·8	15	20	Pure Ar
		17·4			Ar–2·5N_2
		18·0			Ar–5·0N_2
		18·9			Ar–7·5N_2
		19·4			Ar–10N_2
		20·5			Ar–15N_2

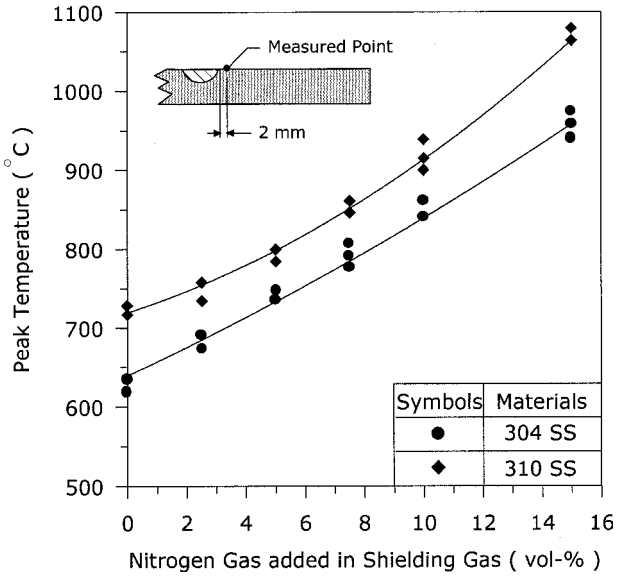

5 Effect of nitrogen gas additions to shielding gas on peak temperature in weldment at 2 mm from fusion line

consistent with the results of investigations by Lin and coworkers.[21–23]

The effect on the arc voltage of nitrogen addition to the argon shielding gas is shown in Fig. 6. The welding current was maintained at a constant value, and it was found that the arc voltage increases as the quantity of nitrogen added to the shielding gas increases. Since the calculated heat input is proportional to the measured arc voltage, added nitrogen

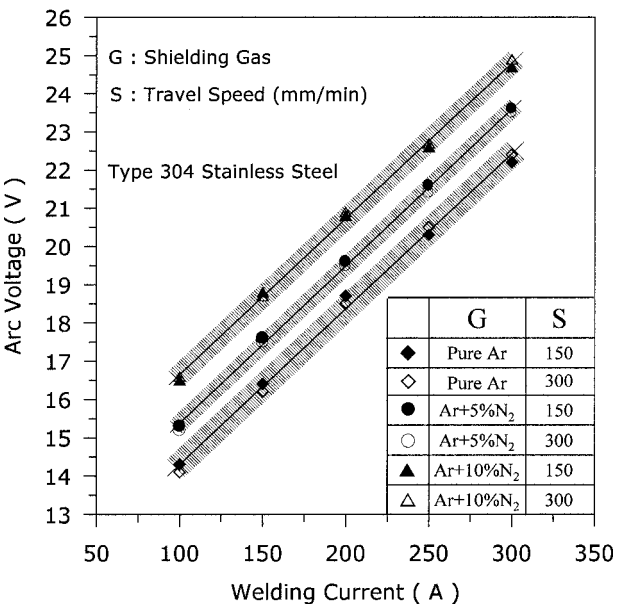

6 Relationship between arc voltage–current curve and volume percentage of nitrogen gas added to argon shielding gas

Table 3 Initial stress evaluation of austenitic stainless steels used

Steel type	Yield stress, MPa	Initial stress, MPa	Stress ratio*, %
304	290	5·9	2·0
310	311	10·6	3·4

*Stress ratio = initial stress/yield stress.

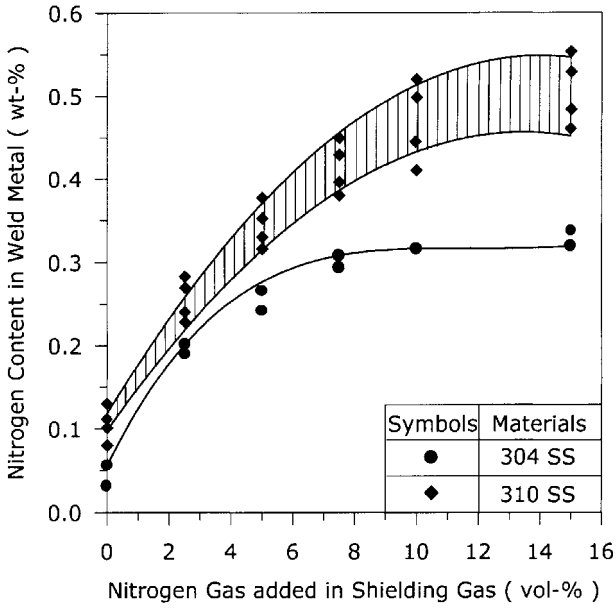

7 Analysed nitrogen content of GTA weld metal as function of nitrogen addition to shielding gas

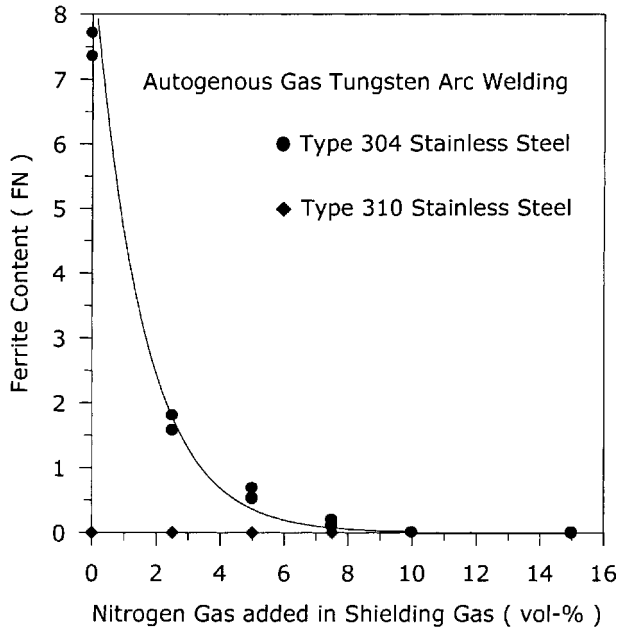

FN ferrite number

8 Measured ferrite content of GTA weld metal as function of nitrogen addition to shielding gas

has the positive effect of increasing the heat input in welding fabrication.

Analysis of nitrogen content in weld metals

The experimental results on the welds of type 304 and 310 stainless steels are presented in Fig. 7. The nitrogen content of the weld metal increases considerably as the added nitrogen in the shielding gas is increased to 15 vol.-%. The nitrogen content becomes saturated at about 0·51 wt-% in type 310 stainless steel weld metals. In type 304 stainless steel weld metals, the nitrogen content in the welds increased with increasing added nitrogen in the shielding gas up to 7·5 vol.-%, beyond which the nitrogen content in the weld metal assumed a constant value of about 0·31 wt-%. In other words, the maximum nitrogen solubility in type 304 stainless steel weld metals is approximately 0·31 wt-%.

It has been reported that nitrogen solubility in weld metal is mainly determined by the heat input and arc length in GTA welding.[13,24] In the present study, since the arc length was kept constant, the nitrogen solubility in the weld metal was determined only by the heat input. As the nitrogen addition to the argon shielding gas increases, the arc voltage is increased. The heat input is therefore also increased. Because this higher heat input can increase the peak temperature of the weld metal and reduce its cooling rate, the amount of nitrogen present in the weld is increased.

The above results clearly indicate that type 310 stainless steel welds can absorb more nitrogen than type 304 stainless steel welds under the same welding conditions. This result can be analysed on the basis of the chemical composition of the materials used. As can be seen in Table 1, the amount of chromium in type 310 stainless steel is higher than that in type 304 stainless steel. Based on the study by Lancaster,[25] the nitrogen solubility increases with increasing chromium content of the materials used. For this reason, the amount of nitrogen absorption in type 310 stainless steel welds is greater than that in type 304 stainless steel welds for the same level of nitrogen gas addition to the argon shielding gas.

Effect of nitrogen addition to shielding gas on retained delta ferrite content in austenitic stainless steel weld metals

The measured ferrite number of weld metals 304 and 310 as a function of nitrogen addition to the shielding gas is presented in Fig. 8. A rapid reduction in measured ferrite number can be seen in weld metals as the nitrogen gas addition to the shielding gas is increased. In type 304 stainless steel welds the ferrite number is reduced to 1·7 FN from its initial value of 7·5 FN by the addition of 2·5 vol.-% nitrogen gas to the argon shielding gas. For 7·5 vol.-% nitrogen gas added to the shielding gas, the retained delta ferrite content in type 304 stainless steel welds can be reduced to near zero. Since nitrogen dissolves interstitially in austenite and is a strong austenite stabiliser, the addition of very small amounts of nitrogen to the argon shielding gas can rapidly reduce the retained delta ferrite content in type 304 stainless steel welds.

The microstructures of type 304 stainless steel welds for different added nitrogen levels are shown in Fig. 9. It can be clearly seen that the retained delta ferrite content in the weld metal decreased with increasing nitrogen addition to the shielding gas. There is a good correlation between the measured ferrite number and metallographic observation of the delta ferrite structure.

It can also be seen in Fig. 9 that an unmixed fusion zone is located adjacent to the base metal along the edge of the weld metal in type 304 stainless steels. In this unmixed fusion zone, the retained delta ferrite quantity always has the predicted value of 7 FN regardless of the volume percentage of added nitrogen gas in the shielding gas. Therefore, the addition of nitrogen gas to the shielding gas does not change the microstructure of the unmixed fusion zone in type 304 stainless steels.

The microstructure of type 310 stainless steel weld metal is fully austenitic at room temperature after solidification. Therefore, the ferrite content does not change (ferrite number is zero) as the nitrogen addition to the argon shielding gas is increased as shown in Fig. 8.

Effect of nitrogen addition to shielding gas on principal residual stress in austenitic stainless steel weldments

Figure 10 shows the maximum principal residual stress in austenitic stainless steel GTA weldments, measured as a

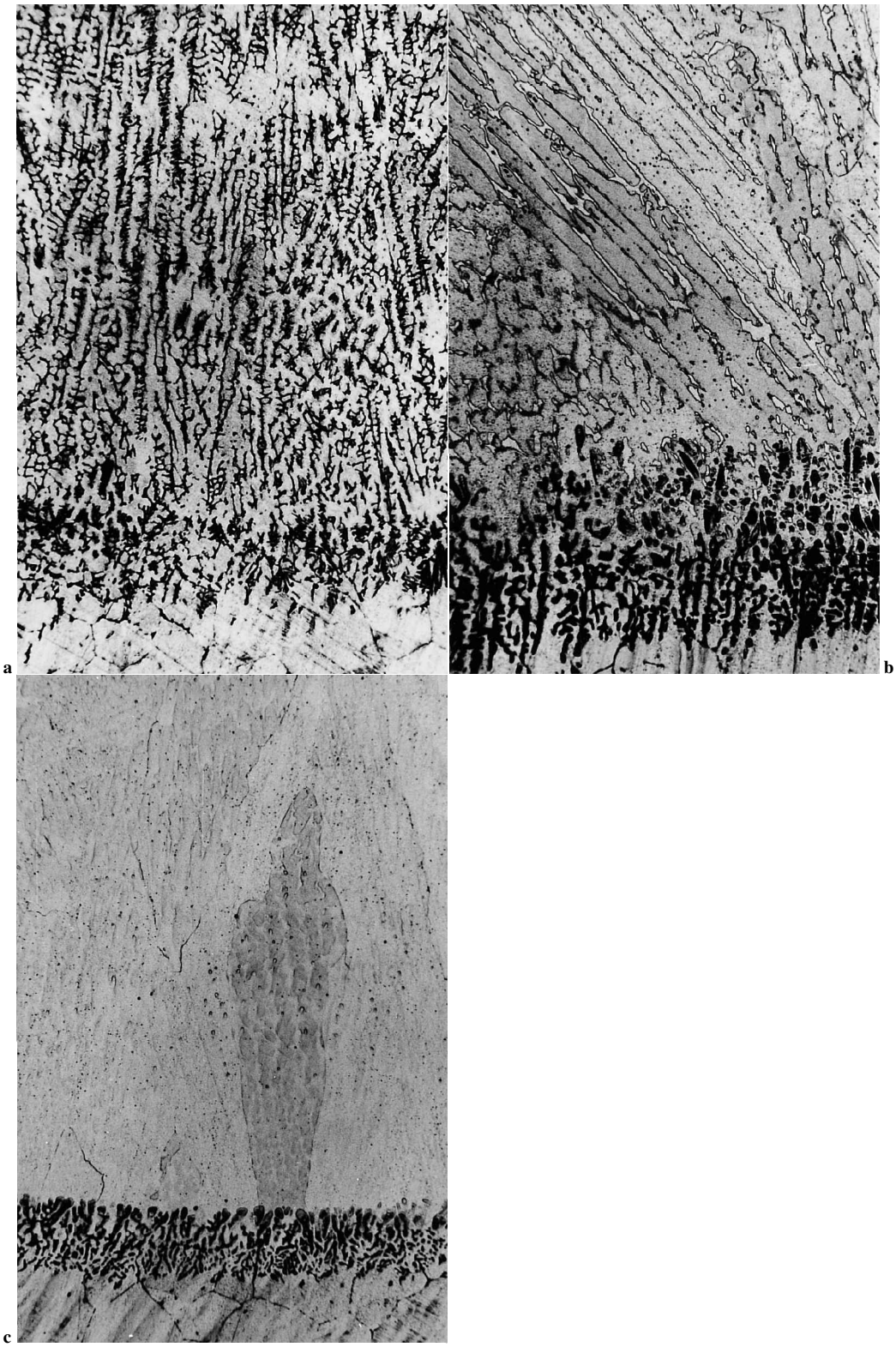

a pure argon (ferrite quantity 7·5 FN); *b* Ar – 2·5 vol.-%N_2 (ferrite quantity 1·7 FN); *c* Ar – 7·5 vol.-%N_2 (ferrite quantity 0·15 FN)

9 Microstructure of type 304 stainless steel weld metal for various shielding gas compositions (optical) × 200

function of the quantity of nitrogen added to the shielding gas. It can be seen that as the nitrogen addition to the argon shielding gas increases, the magnitude of the measured welding residual stress in the austenitic stainless steels is increased. Based on studies by Masubuchi,[26] the welding residual stress increases with increasing heat input. Since the quantity of nitrogen added to the shielding gas increases, the amount of heat input per unit length in a weld can also be increased. Therefore, a higher principal residual stress in austenitic stainless steel weldments can be obtained by the addition of more nitrogen gas to the argon shielding gas in GTA welding.

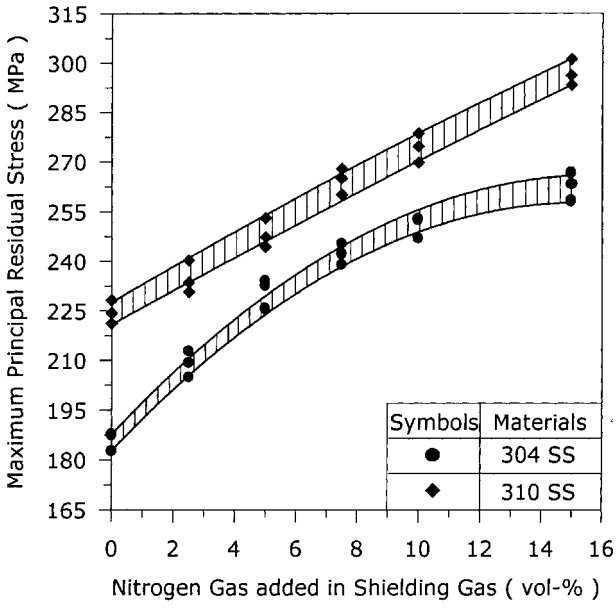

10 Measured residual stress in GTA weldment as function of nitrogen addition to shielding gas

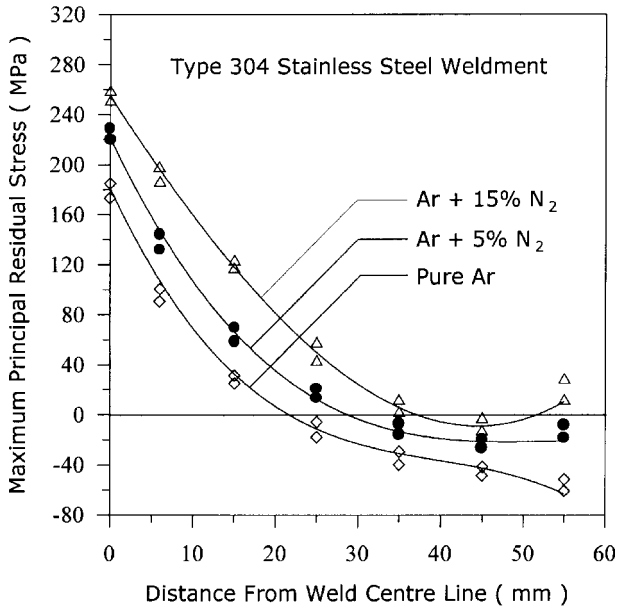

11 Distribution of principal residual stresses in type 304 stainless steel weldments produced via GTA welding

Extent of tensile residual stress zone in austenitic stainless steel weldments

Figure 11 shows the distribution of maximum principal residual stresses in a type 304 stainless steel GTA weldment. It can be seen that as the nitrogen gas addition to the shielding gas increases, the size of the tensile residual stress zone in type 304 stainless steel weldments is extended. According to studies by Masubuchi,[2] the amount of linear heat input is the most significant factor affecting the tensile residual stress zone, which can be extended with increasing welding heat input. Therefore, the greater tensile residual stress zone size in type 304 stainless steel weldments can be obtained via the addition of more nitrogen gas to the shielding gas in GTA welding. The size of the tensile residual stress zone in type 310 stainless steel weldments also can be extended via a similar addition of nitrogen.

In GTA welding, the greater tensile residual stress zone size in austenitic stainless steel weldments is due to the higher heat input and not to the nitrogen content in itself. This is because the nitrogen addition to the shielding gas acts indirectly and actually the welding heat input is the most significant factor affecting the tensile residual stress zone size in weldments.

CONCLUSIONS

1. The addition of nitrogen to the argon shielding gas in GTA welding can increase the heat input.
2. The nitrogen content in austenitic stainless steel weld metals can be increased via increasing nitrogen additions to the argon shielding gas.
3. Adding nitrogen to the shielding gas is an economical and effective method of reducing the retained delta ferrite content in type 304 stainless steel weld metals.
4. An unmixed fusion zone usually occurs in the weld metal near the fusion line if the base metal has a positive delta ferrite potential.
5. The welding residual stress increases with increasing nitrogen addition to the argon shielding gas in GTA welding.
6. As nitrogen addition to the argon shielding gas increases, the size of the tensile residual stress zone in austenitic stainless steel weldments is significantly extended.

REFERENCES

1. C. P. CHOU and Y. C. LIN: *Mater. Sci. Technol.*, 1992, **8**, (2), 179–183.
2. K. MASUBUCHI: in 'Analysis of welded structures', 1st edn, 148–188; 1980, Oxford, Pergamon Press.
3. S. KOU: in 'Welding metallurgy', 1st edn, 109–125; 1987, Toronto, Ont., John Wiley & Sons.
4. K. MASUBUCHI, O. W. BLODGETT, S. MATSUI, F. P. ROSS, C. O. RUDD, and C. L. TSAI: in 'Welding handbook', (ed. L. P. Connor), 8th edn, Vol. 1, 218–264; 1987, Miami, FL, American Welding Society.
5. K. EASTERLING: in 'Introduction to the physical metallurgy of welding', 2nd edn, 1–54; 1992, Oxford, Butterworth-Heinemann.
6. H. KIHARA and K. MASUBUCHI: *Weld. J.*, 1959, **38**, (4), 159s–168s.
7. K. MASUBUCHI and D. C. MARTIN: *Weld. J.*, 1961, **40**, (12), 553s–563s.
8. R. ROBELOTTO, J. M. LAMBASE, and A. TOY: *Weld. J.*, 1968, **47**, (7), 289s–298s.
9. T. TOYOOKA, T. TSUNENARI, R. IDE, and T. TANGE: *Weld. J.*, 1985, **64**, (1), 29s–36s.
10. W. T. DELONG, G. A. OSTROM, and E. R. SZUMACHOWSKI: *Weld. J.*, 1956, **35**, (11), 526s–533s.
11. F. C. HULL: *Weld. J.*, 1973, **52**, (5), 193s–203s.
12. C. J. LONG and W. T. DELONG: *Weld. J.*, 1973, **52**, (7), 281s–297s.
13. T. OGAWA, K. SUZUKI, and T. ZAIZEN: *Weld. J.*, 1984, **63**, (7), 213s–223s.
14. R. H. ESPY: *Weld. J.*, 1982, **61**, (5), 149s–156s.
15. T. ENJO, Y. KIKUCHI, T. KOBAYASHI, and T. KUWANA: *Trans. JWRI*, 1980, **9**, (2), 31–38.
16. T. ENJO, Y. KIKUCHI, T. KOBAYASHI, and T. KUWANA: *Trans. JWRI*, 1981, **10**, (1), 55–62.
17. Y. KIKUCHI, O. KAMIYA, K. KUMAGAI, and I. HIDAYAT: *Trans. JWRI*, 1997, **26**, (1), 109–113.
18. T. WEGRZYN: *Weld. Int.*, 1999, **13**, (3), 173–179.
19. T. OGAWA, S. AOKI, T. SAKAMOTO, and T. ZAIZEN: *Weld. J.*, 1982, **61**, (5), 139s–148s.
20. Standard E387, ASTM, Philadelphia, PA, USA.
21. Y. C. LIN and K. H. LEE: *J. Mater. Process. Technol.*, 1997, **63**, 797–801.
22. Y. C. LIN and J. Y. PERNG: *Sci. Technol. Weld. Joining*, 1997 **2**, (3), 129–132.
23. Y. C. LIN and K. H. LEE: *Int. J. Pressure Vessels Piping*, 1997, **71**, 197–202.
24. J. A. BROOKS: *Weld. J.*, 1975, **54**, (6), 189s–195s.
25. J. F. LANCASTER: in 'Metallurgy of welding', 5th edn, 123–163; 1993, London, Chapman & Hall.
26. K. MASUBUCHI: *Weld. Res. Counc. Bull.*, 1972, **174**, 1–30.